Study of the Influence of Active and Passive Methods for Boundary Layer Control

Milan Matejka
Department of Fluid Dynamics and Thermodynamics
Czech Technical University in Prague, CZ 166 07, Czech Republic
milan.matejka@fs.cvut.cz

Lukas Popelka
Institute of Thermomechanics, Academy of Sciences of the Czech Republic
Prague,CZ 18200, Czech Republic
popelka@it.cas.cz

Presented at the XXVIII OSTIV Congress, Eskilstuna, Sweden, 8 – 15 June 2006

Abstract

The paper deals with the influence of passive and active methods of flow control on the boundary layer of airfoils. Vortex generator type turbulators and synthetic jet actuators were selected for experimental investigation and numerical modeling. Strategies of applications and optimization were introduced and the advantages of adaptive control were briefly discussed on a case of a flapped sailplane airfoil.

Nomenclature

C_f	skin friction coefficient
C_L	lift coefficient
C_p	pressure coefficient
C_μ	total momentum coefficient
c	airfoil chord
f	frequency
F^+	dimensionless frequency
h	orifice diameter
n	ratio of amplitudes of Tollmien-Schlichting waves
Q_{out}	output flow rate
Re	Reynolds number
St	Stokes number
Tu	intensity of turbulence
U	velocity
V_{ac}	applied voltage
X_{te}	dimension of controlled region
x	position
α	angle of attack
γ	angle of flap deflection
ρ	density
ν	kinematic viscosity

Subscripts

B	airfoil bottom surface
inv	inviscid
j	jet fluid
t	turbulator
∞	outer flow
0	mean velocity from the slot

Flow control aims and strategies

The processes within the boundary layer govern the extent of airfoil operational regimes and the performance (depth of laminar bucket). The upper limit at a higher lift coefficient is mainly influenced by turbulent separation. Drag properties are the integral consequences of boundary layer development and the process of transition to turbulence. Turbulence is often coupled with a separation bubble. We are concerned with the Reynolds numbers corresponding to sailplanes.

The flow control methods can significantly affect the airfoil performance by controlling transition and delaying separation. There are several strategies, such as introducing disturbances or vortices to affect the stability of the boundary layer or distribution of momentum within it, etc.

Flow control mechanisms

At first we will summarize which methods can be applied to flow control mechanisms.

Passive methods:

- Surface roughness
- Riblets
- Vortex generators, turbulators

Active methods:

- Steady or unsteady suction
- Steady or unsteady blowing
- Synthetic jet
- Oscillating flap, ribbon, surface
- Acoustic excitation
- Plasma flow control

There are other passive devices, such as Gurney flap and active strategies, e.g. wall heating and cooling, but they are not generally suitable for sailplane use.

The key difference between passive and active methods of the control of shear layers is based on the mechanism of momentum transfer. Applications of passive devices add momentum to the shear layer from the main stream by the modifications of the surface geometry (turbulator, surface roughness, etc.). On the contrary, the active methods require some process or equipment to supply additional momentum to the shear layer. Active methods can be also easily adapted to the varying conditions of the flow (free stream velocity, turbulence intensity, position of separation point, etc.).

Conventional methods of active control are steady suction and blowing, but in comparison with new active methods of control their efficiency is low. A basic idea of up-to-date methods is not only to modify momentum distribution along the thickness of the shear layer, but also to add vortex structures to delay separation. Alternating suction and blowing can be generated using a synthetic jet. Frequency, intensity, direction and magnitude of output momentum from this jet should be optimized in relation to the chorwise dimension of the controlled region, shear layer thickness, outer stream velocity, etc. This principle creates an alternative to the other known devices, such as a oscillating flap (surface), which also generates vortex structures, which in turn affect the character of the shear layer.

Synthetic jet excitation is more effective and efficient than steady blowing or suction [1, 2]. An advantage of this method is zero mass flux supplied to, or taken from the main flow.

There are two possibilities of how to control a boundary layer by synthetic jet actuator (SJA). The first can be called low power control. By application of this method, we can arrange the position of the transition point from laminar to turbulent boundary layer and in the case of a turbulent boundary layer it is possible to delay its separation. This approach requires in-depth knowledge of the physical process and thorough SJA optimization.

The second method is based on the concept of generating a high frequency synthetic jet from the orifice, similar to the continuous jet. The main issue is to construct a SJA with sufficient power output.

The intensity of a synthetic jet is determined by the total momentum coefficient [3, 4]:

$$C_\mu = \frac{\rho_j U_j^2 h}{1/2 \rho_\infty U_\infty^2 c} \qquad (1)$$

where U_∞ and ρ_∞ are the velocity of the outer flow and the fluid density, respectively, U_j, ρ_j are the same quantities related to jet fluid, h is the jet orifice diameter or width of slot, c is the characteristic dimension of the body. Typical values of the total momentum coefficient range from 0.1% to 3% for synthetic jet boundary layer control.

To characterize the operation of the SJA, the following relationships can be formulated:

dimensionless frequency F^+

$$F^+ = \frac{f \cdot X_{te}}{U} \qquad (2)$$

Reynolds number (for the orifice)

$$\mathrm{Re}_0 = \frac{U_0 \cdot h}{\upsilon} \qquad (3)$$

Stokes number (for the orifice)

$$St = \frac{f \cdot h^2}{\upsilon} \qquad (4)$$

where f is the actuated frequency, X_{te} is the dimension of the controlled region (such as distance between actuator and trailing edge), U is the free stream velocity, h is the width of slot and U_0 is the mean velocity from the slot.

The optimum of the dimensionless frequency F^+ has been determined in previous research works to fit into the interval from 1 to 10. We should point out that the change of F^+ strongly affects the minimum of the total momentum coefficient, which is capable to control the flow. Values of St are influenced as well and optimum results are obtained for values of $St < 10$.

Synthetic Jet Actuator

The SJA is designed as a cavity with a periodically moving boundary and an orifice or slot which generates a jet of fluid (see also Ref. 3, 5, 6). Figure 1 shows the scheme of the flow in the proximity of the orifice. There exist two main directions of the flow caused by two phases of the jet. Orientation of the first one, blowing, is along the central line of the orifice. The second phase, suction, brings air along the wall into the orifice.

Synthetic Jet Actuator design – Lumped Element Model (LEM)

At relatively low frequencies, where the characteristic length scales of the physical phenomena are larger than the largest geometric dimension, the governing partial differential equations of the dynamic system of the synthetic jet actuator can be easily transferred into a set of coupled ordinary differential equations. Individual parts of the actuator components are modeled as elements of an equivalent electrical circuit using conjugate power variables. The frequency response function of the circuit is derived to obtain an expression for Q_{out}/V_{ac}, the volume flow rate to applied voltage. The idea of the LEM has been introduced in Ref. 5 and 6, where detailed derivation of the model is also shown.

The change of various SJA parameters (width of slot, volume of cavity, properties of membrane, etc.) significantly affects the dynamical behaviour, the amplitude-frequency response and the velocity amplitude of the output fluid flow.

The presented model enables the optimization of the SJA parameters to obtain maximum output velocity or momentum of the flow and a wide frequency range with high velocity output etc.[6]. However, there are problems to estimate the constants. For example, it is difficult to estimate the material constants as an impact of the wall acoustic rigidity. It is necessary to verify the constants experimentally.

Experimental setup

The general-purpose, closed-circuit wind tunnel of 750x550mm cross section of the Czech Technical University (CTU) was used with wind tunnel models with end plates located in an open test section. Particle Image Velocimetry (PIV) measurement, pressure distribution acquisition and smoke-wire visualization were applied. Additional measurements were carried out in a 2D 1200x400mm wind tunnel.

The passive method of transition from laminar to turbulent boundary layer control was studied experimentally on airfoil PW212-163 shown Fig. 2 (the design of the airfoil is given in Ref. 7). Investigation was particularly aimed to the extent of laminar separation with respect to the turbulator position.

The active method of boundary layer control was experimentally tested on the simplified airfoil model with flap. To achieve flexible layout and easy access to actuators, simple geometry was chosen. The position of the actuators and main dimension of the model are depicted in Fig. 3. The angle of flap deflection γ was varied from 22 to 26 degrees.

In the first test case, the SJA equipped with piezoceramic membrane was used. The LEM method described earlier was applied for the SJA design. A slot of 0.5 mm width was used as the output orifice. The SJA was placed perpendicular to the surface in the region of the leading edge, position 1 on Fig. 3. The output velocity was measured at a distance of 0.5 mm above the slot by hot-wire in CTA (Constant Temperature Anemometry) mode. Calculated and measured amplitude-frequency characteristics are shown in Fig. 4 for the amplitude of the actuating voltage of 15V. The maximum of the synthetic jet mean velocity was over 25 m/s for frequencies of 2600 and 3800 Hz.

The second case represents the same wind tunnel model. The boundary layer has was controlled by two SJA based on the electrodynamic actuators (speakers) of 52 mm diameter in positions 2 and 3. Both SJA have five output orifices, which are located in line along the span of the model, with distances of 4 mm. The amplitude-frequency characteristic of the actuator was obtained experimentally using hot-wire anemometry in CTA mode. The amplitude of the actuating voltage was 2V. The corresponding amplitude-frequency characteristic of the actuator is plotted in Fig. 5. The maximum of the synthetic jet mean velocity 1mm above the orifice was 11 m/s at a frequency of 300 Hz.

Results

Digital images of smoke-wire visualizations of the passive control test case on airfoil PW212-163 are shown in Fig. 6. Three positions of lower-surface-installed standard zig-zag turbulator of 0.5 mm height are presented. Boundary layer laminar separation, transition to turbulence, turbulent reattachment and elimination of the separation bubble for optimum device application are demonstrated. Due to the vortices introduced by the tape in the position $x_{tB}/c = 0.5$, the transition is finished upstream of the region of steep pressure gradient, which is overcome by the turbulent boundary layer without separation. Experimental data were obtained for free stream conditions $Re = 2.1 \cdot 10^5$ and turbulence intensity $Tu = 1.3\%$. Numerical simulation was done for the same parameters using Xfoil airfoil analysis code[8]; the results are in Fig. 7. Corresponding pressure distribution measurements proved elimination of the separation bubble for the whole range of design lift coefficients. Nevertheless, single element airfoil geometry with lower surface fixed transition created performance restrictions.

Experimental results of the first test case of active boundary layer control are presented in Fig. 8. On the upper part, the uncontrolled flow field is shown; the separation bubble can be clearly seen. On the lower part, the flow field controlled by the SJA is shown. Generated vortex structures accelerated the transition from laminar to turbulent boundary layer and the extent of the separation bubble has been reduced.

The second SJA experiment is focused on the delay of boundary layer separation; electrodynamic actuators were used. Measured velocity profiles are presented in Figs. 9 and 10 for the given free stream velocity. There are large differences between the actuated and unactuated flow field. Flow control efficiency depends on the velocity ratio of the free stream flow and synthetic jet. Lower synthetic jet output velocity compared to the free stream velocity cause a thicker wake behind the flap. Also, a strong effect of direction of the jets is apparent on the velocity profiles. For optimal design of the synthetic jet, the reduction of the synthetic jet angle to the surface or application of Coanda effect would be suitable.

In Fig. 11, the fields of vorticity for an angle of flap $\gamma = 22$ deg at free stream velocity 3.7 m/s are depicted. There is a clear change of the intensity of the vorticity field, which is caused by the actuator on the flap. It is evident that the rate of aero-shaping depends on the proportion of free stream and synthetic jet velocity.

Application of passive, active and adaptive flow control on sailplane airfoils

Control of the transition by passive methods or steady blowing is limited to one prescribed position and, with this constraint, the design of airfoil contour and flow control has to be carried out, as shown on PW212-163 airfoil, Fig. 6 and 7. The possibility of detrimental separation bubble elimination by active flow control on a simplified airfoil with flap is shown in Fig. 8.

The other important issue for flow control is turbulent separation arising in the flow field due to landing flap deflection, but also in some cases on ailerons in climb within thermals. Feasibility of momentum supply close to the surface

and, hence, enabling the delay of boundary layer separation is presented in Figs. 9, 10 and 11.

Advantages of adaptive control can be demonstrated on a flapped airfoil as also shown in Ref. 9. DU type airfoils are representative of contemporary high-performance sailplanes. According to the published pressure distribution[11], contour was calculated by means of an inverse iterating method.

Flap setting and Reynolds number - corresponding to interthermal glide and circling in thermal - change the conditions for the boundary layer on the lower surface significantly. With use of numerical modeling, it can be shown that there is a wide range of required positions of turbulent boundary layer onset to prevent separation bubbles as depicted in Fig. 12. A passive transition control device, placed in the optimum location for flap deflection $\gamma = 20$ deg at location x/c = 0.65, would cause a large drag increase for $\gamma = 0$ deg, where laminar flow up to x/c = 0.95 can be achieved. A synthetic jet with adjustable frequency could be a prospective device for the adaptive transition control required in this case. Since airspeed and flap setting have significant effect on boundary layer development, they could be used as the primary triggers for the actuator system.

The proposed control strategy could be applied on the upper airfoil surface as well, but the detrimental effect of separation bubbles for a large range of angles of attack and flap settings can be eliminated by careful contour design[11]. A different situation would arise with large (landing) flap deflection, where the airfoil lift coefficient is limited by turbulent boundary layer separation. In this case, suitable flow control can be apparently beneficial.

Although power consumption of the presented piezo-driven and electrodynamic actuators is low, there is another feasible way of generating the synthetic jet by steady blowing and appropriate acoustic design of the cavity and orifice. That possibility is more suitable for sailplanes, since the needed supply of pressure air can be obtained by pitot tube(s) or NACA inlet(s).

Conclusion and future work

In the case of passive control, the importance of proper application of turbulator tape has been highlighted. Coupled with airfoil design, it is possible to find desired optimal device dimensions and position, which covers the required range of operating conditions, but an adaptive control cannot be reached.

The potential of an active method of flow control is more extensive, but also more complicated to design. Function of the synthetic jet actuator depends on a set of design parameters, such as dimensionless frequency F^+, total momentum coefficient c_μ, etc. and an optimum combination is sought.

In the first presented test case, the following design parameters were used: $F^+ = 145$, $c_\mu = 0.04$, $Re_0 = 560$ and St = 40. Some of these parameters are not within their ideal range, but an effect on the boundary layer was obtained. The main reason is a high value of c_μ. For higher efficiency of control, it would be better to reduce F^+.

The second test case was operated with these parameters: $F^+ = 17$ +/- 42, $c_\mu = 0.02$ +/- 0.09, $Re_0 = 340$ and St = 4.7 (for one orifice). There are considerable impacts of the synthetic jet to the thickness of the boundary layer; the direction and the intensity of the synthetic jet have noticeable effect to the shape of the velocity profile.

The relative chordwise position of SJA to the separation region is essential, which has been verified on three available locations. It is possible to virtually shape the surface using the synthetic jet actuator, but it is necessary to use high power actuators and to define the control process of the actuators.

Future work will be focused on design of SJA applicable to the real conditions.

Editor's comment: The following questions resulted from the review process. The authors provided answers just before press-time:

What is the power required for the synthetic jet? The power requirement for one synthetic jet (SJA) applied in tests was 250 mW. A noticeable effect on the boundary layer was observed in width of 80 mm along the span of the model. For example, the system of such efficiency when installed on 15 m sailplane would require 45 W of power.

What are the detrimental effects of passive devices when operating off-design point? An example of such a case is presented in Fig. 12 on a DU type flapped airfoil. Two flap deflections corresponding to lift coefficients of $c_L = 1.2$ and $c_L = 0.3$, $\mathrm{Re}\cdot\sqrt{c_L} = 10^6$ are considered. Theoretical optimum location of transition flow control device for low-speed flap deflection γ = 20 deg is at location x/c = 0.65. Applying a passive device (e.g. turbulator tape) in this position would cause a high-speed setting of $\gamma = 0$ deg and a drag increase in order of 20%, which is unacceptable.

Which surface was tested in Fig. 3? The outer (upper) surface of the body was tested.

How would the active flow control device be switched on/off? In the case of a electrically powered SJA, the supply of electric power would be switched on/off. A more suitable possibility would be to generate the synthetic jet by steady blowing and appropriate acoustic design of the cavity and orifice. This option has been mentioned as feasible and a detailed study is now underway. The straightforward control of the device would be by switching on/off the supply of pressure air, i.e. by closing a valve on the intake from the pitot tube/NACA inlet.

What was the actuation frequency in Fig. 8? Actuation frequency was 2640 Hz.

Does the actuation frequency need to be matched to the flow conditions? For both cases concerning boundary layer transition and turbulent boundary layer separation, the frequency must be well matched to the flow conditions.

Is the SJA orifice a circular hole, or an extended slot? The output orifice of the SJA in position 1 is an extended slot. In position 2 and 3, five circular holes are located in line along the span of the model. Both types of output orifices can be used to control the boundary layer transition. For control of turbulent layer separation, it is more efficient to use an extended slot as the output orifice.

Acknowledgment

The work has been supported by the project of Progressive Technology System for Power Engineering 1M06059, by the Ministry of Education, Youth and Sports No. 1M06031, also grant support of GA AS CR No. IAA2076403, No. IAA200760614 is gratefully acknowledged.

References

[1] Smith, B.L., Swift, G.W.: *A comparison between synthetic jets and continuous jets*. Experiments in Fluids 34 (2003) 467–472, 2003

[2] Mittal, R., Rampunggoon, P., Udaykumar, H. S.: *Interaction of a Synthetic Jet with a Flat Plate Boundary Layer*. AIAA 2001–2773, 2001

[3] Glezer, A., Amitay, M.*: Synthetic Jet*. Annu, Rev. Fluid Mech. 2002

[4] Uruba, V.: *Flow Control Using Synthetic Jet Actuators*. Engineering Mechanics 2004, pp. 25-26. ISBN 80-85918-88-9

[5] Gallas, Q, Mathew, J. Kaysap, A., Holman, R., Nishida, T., Carroll, B., Sheplak, M., Cattafesta, L.: *Lumped Element Modeling of Piezoelectric-Driven Synthetic Jet Actuators*. AIAA 2002-0125, 2002

[6] Gallas, Q., Wang, G., Papila, M., Sheplak, M., Cattafesta, L.: *Optimization of Synthetic Jet Actuators*. AIAA 2003-0635, 2003

[7] Popelka L.: *PW series airfoils - numerical optimization and wind-tunnel measurement*, Proceedings Colloquium Fluid Dynamics, Institute of Thermomechanics AS CR, Prague, 2005, pp. 117-120

[8] Drela, M., Youngren, H.: *Xfoil 6.9 User Guide*, MIT, 2001, URL: http://raphael.mit.edu/xfoil/ [cited 1 May 2006]

[9] Sartorius, D., Würz, W., Wagner, S.: *Experimentelle Untersuchung zur Kontrolle laminarer Ablöseblasen*, Institut für Aerodynamik und Gasdynamik, Universität Stuttgart, 2002, URL: http://www.iag.uni-stuttgart.de [cited 1 May 2006]

[10] Boermans, L.M.M., Van Garrel, A.: *Design and Windtunnel Test Results of a Flapped Laminar Flow Airfoil for High Performance Sailplane Applications*, Technical Soaring, Vol. 21, No. 1, 1997, pp. 11-17

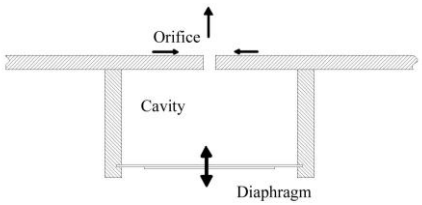

Figure 1 Synthetic jet - scheme of the flow

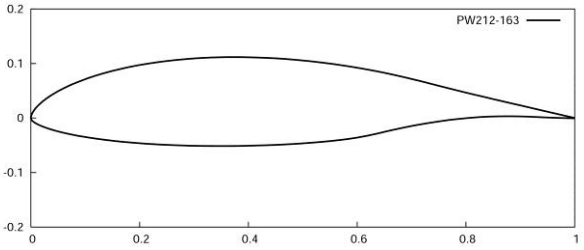

Figure 2 Contour of the PW212-163 airfoil

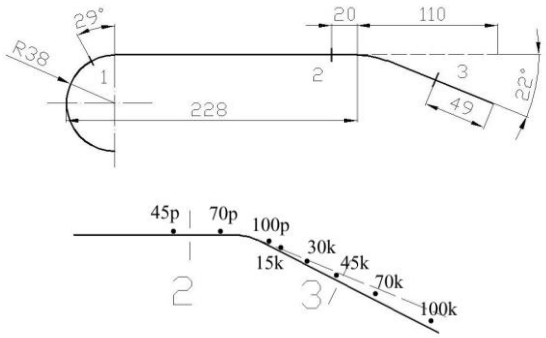

Figure 3 Main dimensions of simplified airfoil with flap, locations of synthetic jet actuators (1-3) and measured velocity profiles positions

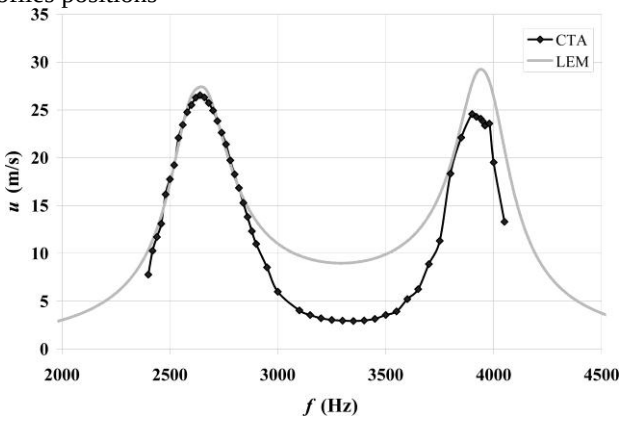

Figure 4 Amplitude [u (m/s)]-frequency [f (Hz)] characteristic of piezo-actuator, LEM calculated data and CTA measurement

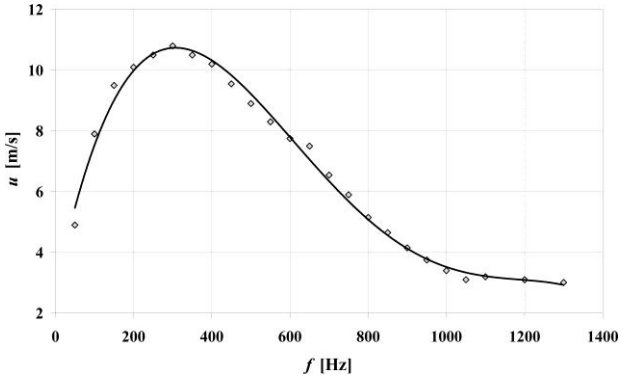

Figure 5 Amplitude [u (m/s)]-frequency [f (Hz)] characteristic of electro-dynamic actuator

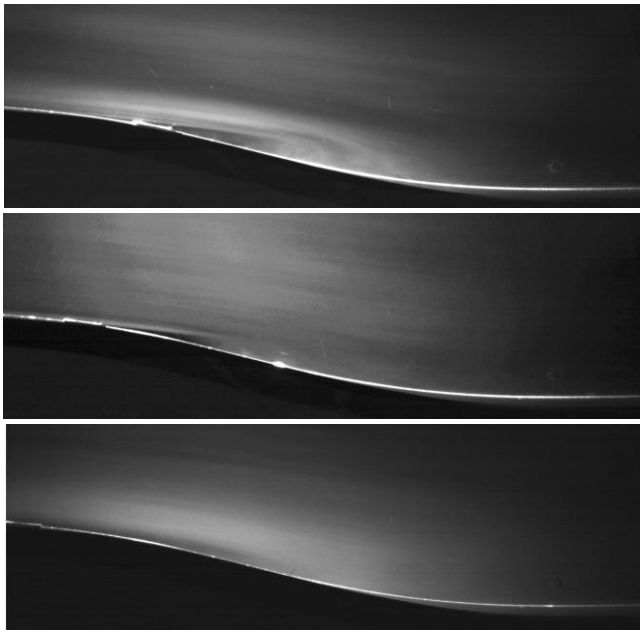

Figure 6 Airfoil PW212-163, Re = $2.1 \cdot 10^5$, Tu = 1.3%, □ = 0 deg. Boundary layer visualization, positions of turbulator, top to bottom: x_{tB}/c = 0.6, x_{tB}/c = 0.55 and x_{tB}/c = 0.5, elimination of separation bubble

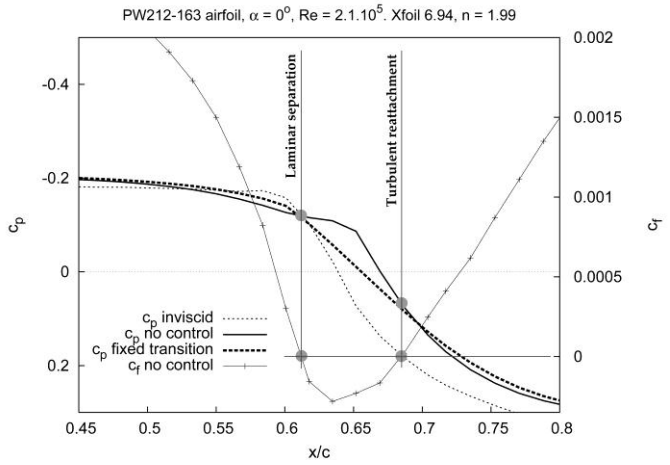

Figure 7 Airfoil PW212-163, free stream conditions Re = $2.1 \cdot 10^5$, Tu = 1.3%, α = 0 deg. Calculated pressure distribution and skin friction coefficient on lower surface, Xfoil 6.94

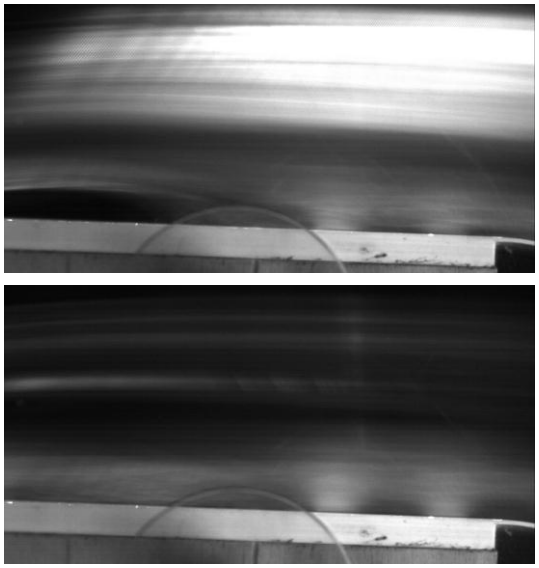

Figure 8 Active control visualization on upper surface of model plate with flap. Upper figure – not actuated case, note separation bubble on the left side, lower figure – actuated case, attached boundary layer. Free stream conditions Re = 100 000, Tu = 1 %, piezoceramic SJA in position 1

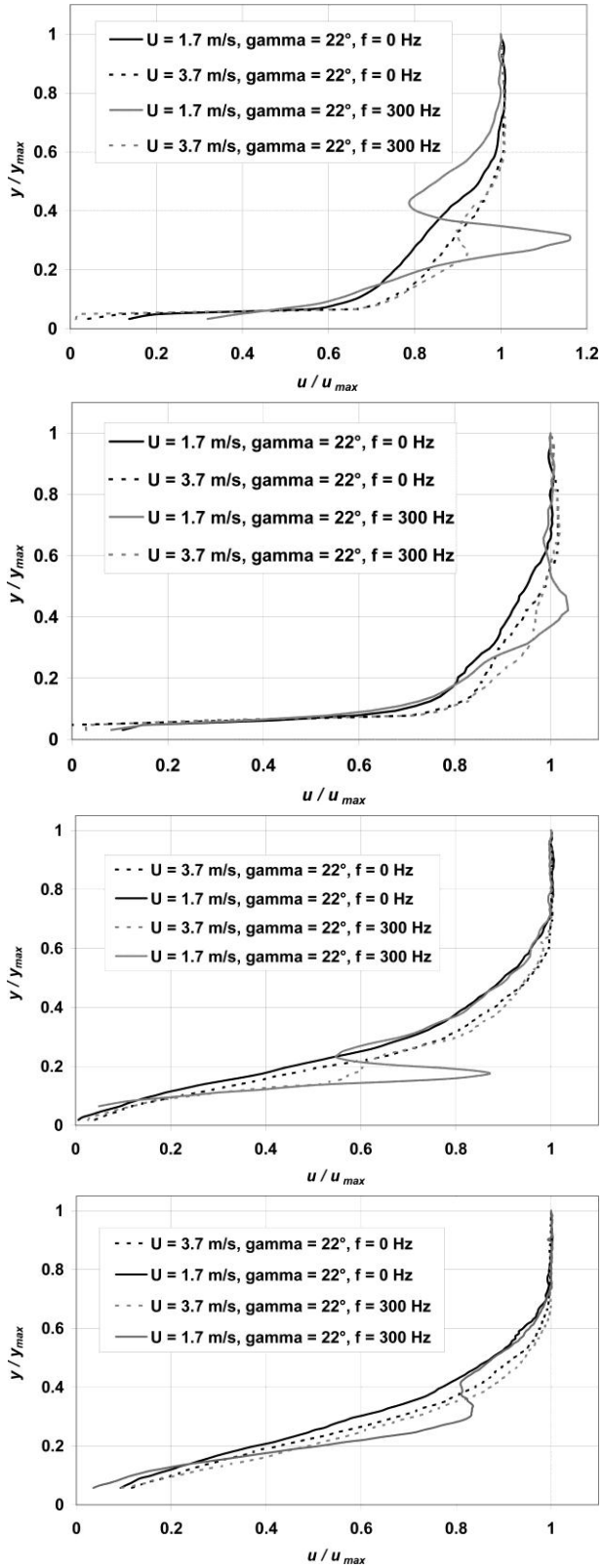

Figure 9 Normalized velocity profiles on model plate with flap, chordwise location top to bottom: 70p, 100p, 70k, 100k. Electrodynamic SJA in positions 2 and 3

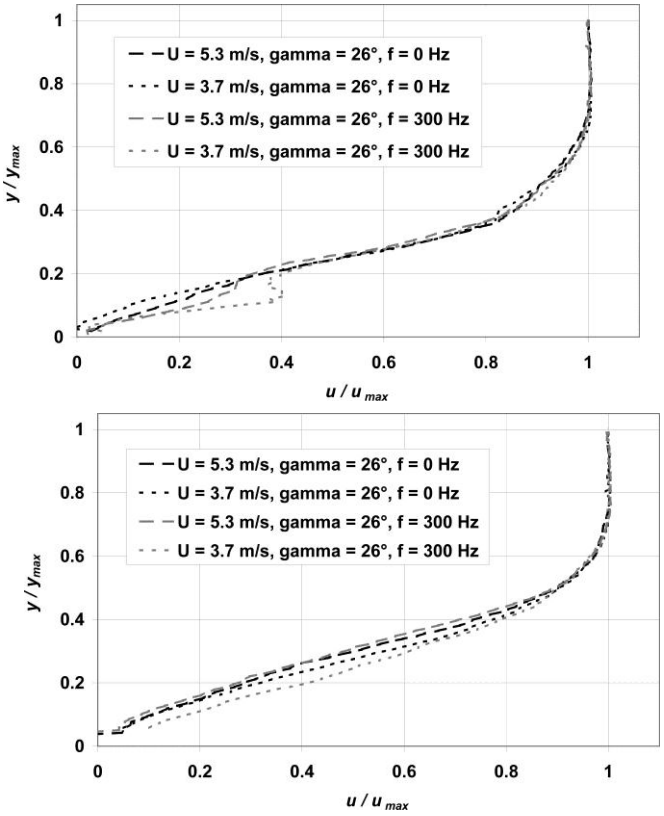

Figure 10 Normalized velocity profiles on model plate with flap, chordwise location top to bottom: 70k, 100k. Electrodynamic SJA in positions 2 and 3, angle of flap $\gamma = 26$ deg

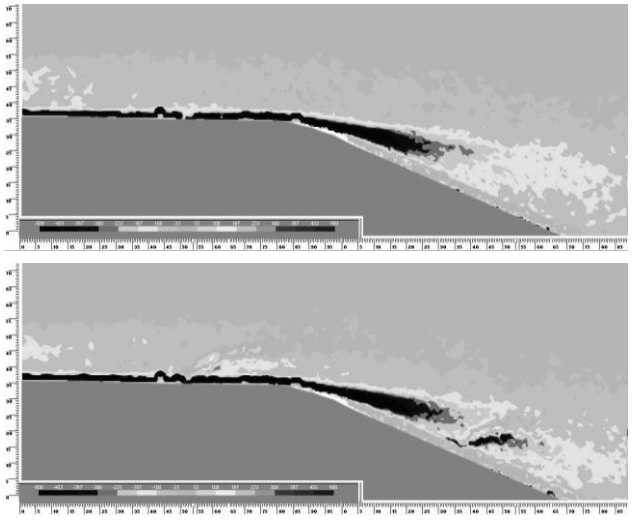

Figure 11 Vorticity field, Re = 80000, angle of flap $\gamma = 22$ deg, lower figure shows flow field with synthetic jets

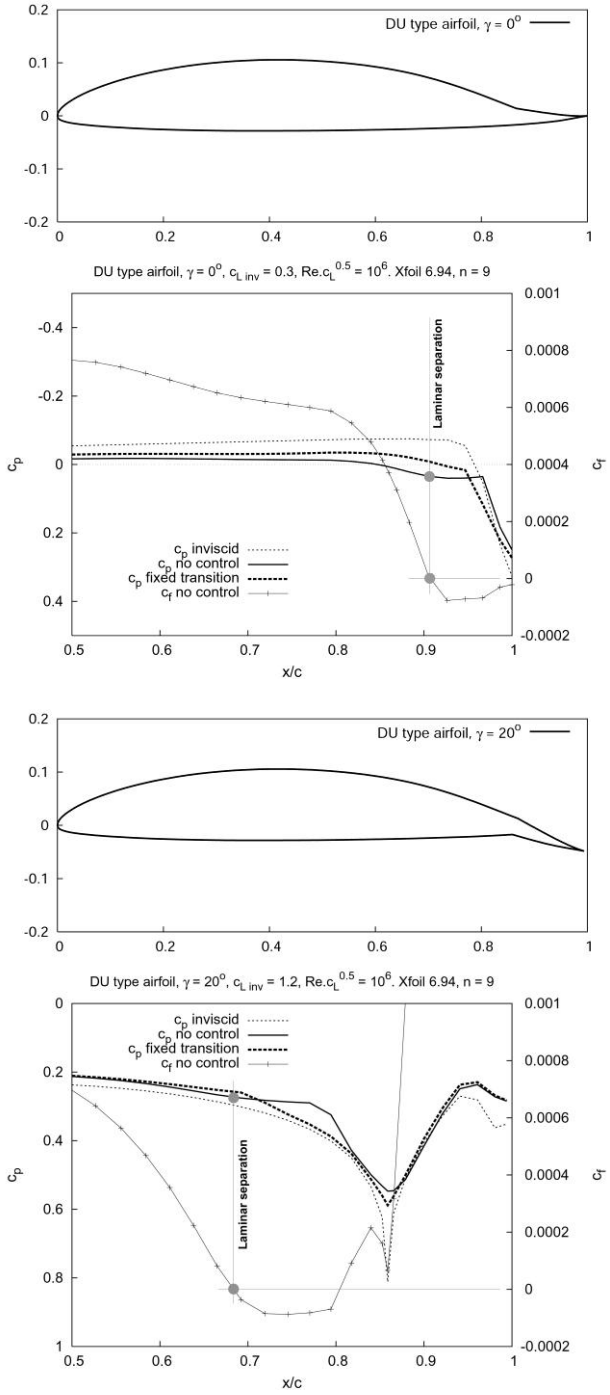

Figure 12 Contour of flapped airfoil for flap deflection $\gamma = 0$ deg and $\gamma = 20$ deg, calculated pressure distributions and skin friction coefficient on lower surface. Location of laminar separation onset for case without boundary layer control, Xfoil 6.94